Exergy Analysis of the Process for Dimethyl Ether Production through Biomass Steam Gasification

ARTICLE *in* INDUSTRIAL & ENGINEERING CHEMISTRY RESEARCH · DECEMBER 2009

Impact Factor: 2.59 · DOI: 10.1021/ie900199e

5 AUTHORS, INCLUDING:

X.P. Zhang
Chinese Academy of Sciences
167 PUBLICATIONS **2,654** CITATIONS
SEE PROFILE

Christian Solli
Independent Researcher
28 PUBLICATIONS **349** CITATIONS
SEE PROFILE

Edgar G. Hertwich
Norwegian University of Science and Tech…
167 PUBLICATIONS **4,814** CITATIONS
SEE PROFILE

Exergy Analysis of the Process for Dimethyl Ether Production through Biomass Steam Gasification

Xiangping Zhang,*,†,‡ Christian Solli,† Edgar G. Hertwich,† Xiao Tian,‡ and Suojiang Zhang‡

Industrial Ecology Programme and Department of Energy and Process Engineering, Norwegian University of Science and Technology (NTNU), NO-7491 Trondheim, Norway, State Key Laboratory of Multi-Phase Complex System, Institute of Process Engineering, Chinese Academy of Sciences, Beijing 100190, China

A flowsheet for the production of the substitutable transportation fuel dimethyl ether through biomass steam gasification to fuel (BSGtF) was constructed including heat integration. A quasi-equilibrium model was applied to simulate the whole process based on rigorous thermodynamic property prediction models. The carbon and hydrogen flows of the process showed that the atom utilization efficiency of carbon from the biomass to fuel process was 38.47%, and 39.75% of the total hydrogen was converted to the fuel product. The exergy flows of the total process and the exergy loss taking place in each process section were calculated based on the second law of thermodynamics. The results indicated that the total energy and exergy efficiencies from biomass to fuel were 51.3% and 43.5%, respectively, with a negative CO_2 emission effect. The effects of gasification temperature, combustion temperature, and steam/biomass ratio on the gasification performance were investigated. The causes of exergy losses were analyzed to identify the areas of improvement so that a high energy utilization efficiency could be achieved.

1. Introduction

Transportation currently relies on oil for virtually all of its fuel and comprises one-half of world oil consumption. This accounts for about 20% of the total CO_2 emissions from the transportation sector worldwide. With the evident shortage of oil reservoirs, producing transportation fuels from other resources, such as natural gas, coal, or biomass through syngas, has become an attractive alternative, as it would not necessitate a change in the existing infrastructure using hydrocarbon fuel. Producing transport fuel with fossil fuel resources, such as coal, could relieve the crude oil crisis, but from the perspective of long-term sustainable development, depletion of nonrenewable resources and concerns about global warming are shifting the focus from carbon-rich fossil fuels to carbon-neutral fuels, which would also provide a "road map" to decarbonization.[1]

As a carbon-neutral resource, biomass is considered to be the only renewable source of industrial petrochemical feedstocks and fuels for transportation that cannot be provided by electricity.[1] Therefore, producing transportation fuel from biomass (biofuel) is a prospective path toward transportation fuel sustainability and can offer a chance to turn bioenergy into a carbon-negative industry, which can be a good solution both for fossil fuel depletion and for global warming. Additionally, compared to fossil fuel resources, biomass such as wood has low nitrogen and sulfur contents, and hence, its controlled emissions (such as SO_x and NO_x) are extremely low.

One promising technology for producing biofuel is synthesizing hydrocarbon fuel through syngas, which is produced by biomass gasification. Furthermore, roughly one-third to one-half of the amount of CO_2 that is released during the biofuel synthesis process can be captured and stored, which results in so-called negative CO_2 emissions considering the total life cycle of the biomass to transportation fuel. Detailed descriptions of the gasification mechanism, tar control, gas cleaning, operating conditions, and pilot-scale tests are available in the literature.[2−5] Recently, pure steam gasification has received increased attention and has been found to have many advantages.[6−9] Compared to gasification with air or oxygen, steam gasification requires no O_2 separation and it has a N_2-free product gas, a medium-heating-value (10−18 MJ/Nm^3) gas product, and a composition with more H_2 and CO and less CO_2. Research has also shown that the commercial version of this process is likely to have a very high carbon conversion (99.9%), which makes this technology favored by industrial institutions, such as Battelle.[10,11] The high H_2 and CO contents in syngas are especially beneficial for producing chemical fuel or H_2. Nevertheless, pure steam gasification needs indirect heating, which makes this process relatively complicated. Because it requires combustion of byproduct char (or other additional fuels) in a second reactor where heat is carried by the circulating sand, the heat balance between gasifier and combustor with maximum thermal efficiency should be optimized.

As a new and substitutable fuel, dimethyl ether (DME) promises to be a low-carbon and medium-term alternative fuel to diesel or liquefied petroleum gas, because of its low NO_x, SO_x, and hydrocarbon emissions,[12−15] as well as the use of renewable feedstocks for its production. For example, the CO_2 emission indexes for DME and Fischer−Tropsch (F−T) diesel are 0.0662 and 0.07312 kg of CO_2/MJ heat (LHV), respectively; thus, the use of DME as fuel supports the use of diesel engine vehicles with lower CO_2 emissions than F−T diesel. Moreover, DME is a chemical feedstock for producing light alkenes, and because it is easily transported, it is suitable for generating H_2 for automotive fuel cells. In this work, we selected DME as the final simulated fuel product.

Although many advantages of biofuels have been realized and many new technologies have been investigated in the laboratory at a relatively small scale, the lack of knowledge on process assessments and predictive abilities for those new processes might cause potential failures in industrial applications. Hence, understanding the global performance and behavior of the conversion of biomass to transportation fuel and assessing the total process in terms of both energy efficiency and

* To whom correspondence should be addressed. E-mail: xpzhang@home.ipe.ac.cn. Tel./Fax: 86-10-62558174.

† Norwegian University of Science and Technology (NTNU).

‡ Chinese Academy of Sciences.

10.1021/ie900199e CCC: $40.75
Published on Web 11/09/2009

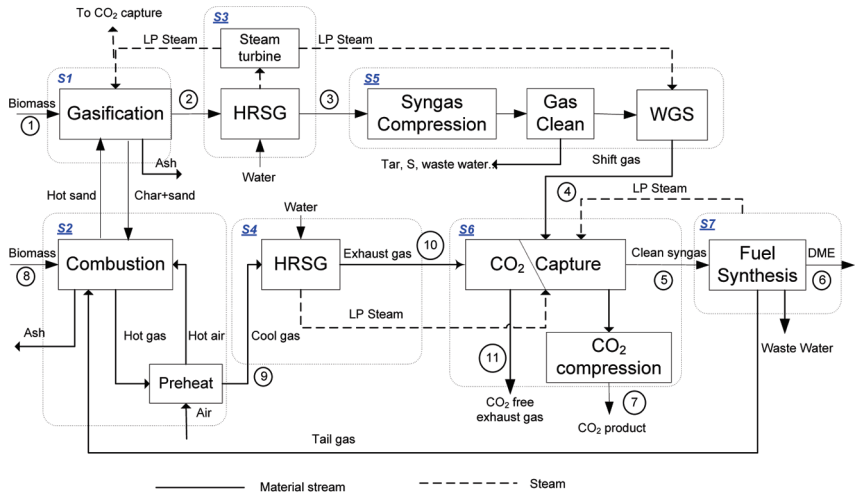

S1 — Gasification process; *S2* — Combustion & air preheat; *S3* — Heat recovery of raw syngas;

S4 — Heat recovery of combustion flue gas; *S5* — Gas compression & water gas shift;

S6 — CO_2 capture & compression; *S7* — DME synthesis

HRSG: Heat Recovery Steam Generation

Figure 1. Principal flowsheet of BSGtF process with heat integration.

technological feasibility are significant prerequisites. However, not much research has been published in this area, especially concerning rigorous process models. One of the main reasons for this lack is that the complicated biomass feedstock composition and extremely complex thermodynamics and reaction models make such assessments difficult. Therefore, simplified correlation or equilibrium models have often been recommended to simulate the biomass gasification process in the literature,[8,16−20] and the deviations from experimental values were verified with the correlated formulas. Prins et al. discussed the feasibility of equilibrium models for describing gasification and reviewed the existing associated works.[17] They concluded that one effective model is a quasi-equilibrium model that uses the quasi-equilibrium temperature, whereby the equilibria of the reactions defined in the models are evaluated at a lower temperature than the actual process temperature depending on the different configurations of the gasifier, around 100−300 °C.[17,21]

Some other works have also related to the process assessment of biomass to fuel or power. The possibilities for the production of F−T liquids and power via biomass gasification were investigated by Tijmensen et al., covering the technological feasibility and economics of different configurations.[8] Detailed modeling and analysis of biomass gasification was, however, not included. The exergetic optimization of a production process of F−T fuels from biomass was studied by Prins et al., and their recommendations for process improvements were based on a simulation approach and overall exergetic efficiency.[18] Their study assessed the air-blown autothermal biomass gasification at atmospheric pressure (directly heated), using the once-through mode. Both the F−T fuel and electricity were designated as final products. The above works have provided important references for developing new biomass utilization technologies. Moreover, it has been acknowledged that developing a deep understanding of the mechanisms of material and energy conversion in the constructed flowsheet and in the single units by using energy and exergy analyses based on simulation technology and rigorous estimation of the thermodynamic properties is vital in the planning and design of the future carbon-constrained transportation fuel production process.

In this work, a biomass-to-DME flowsheet configuration through biomass steam gasification was constructed with full conversion of syngas to DME by recycling the unreacted reactants in the DME synthesis process. The material and energy information of the main streams, the carbon and hydrogen flows of the process, were predicted, and energy and exergy analyses of this process were performed based on the rigorous simulation results. The goal of energy and exergy methods in engineering is to calculate the balances between what comes into and goes out of several possible designs before a factory is built. An energy efficiency or first-law efficiency will determine the most efficient process based on losing as little energy as possible relative to energy inputs. An exergy efficiency or second-law efficiency will determine the most efficient process based on losing and destroying as little available work as possible from a given input of available work, and also the causes of exergy losses were analyzed, and the improvement measures can be proposed.

2. Process Construction and Description

A configuration of the indirect biomass steam gasification to fuel (BSGtF) process including heat integration is shown in Figure 1. The principal flowsheet and operating parameters of the gasifier and the combustor were determined using data for the low-pressure indirect biomass gasification technology of Battelle Columbus Laboratory (BCL),[11,22] as well as experimental data.[6] The biomass gasifier heats the biomass in a chamber filled with hot sand (or olivine[6]) until the biomass breaks down into its constituent chemical components. The solid, sand, and char are separated from the constituent gases while being passed through a scrubber. To reduce equipment size and, hence, cost to satisfy the further processing requirements, the syngas from the gasifier is pressurized after cooling for further processing including the water−gas shift (WGS) reaction, CO_2 removal, and fuel synthesis; the technologies of these downstream units are relatively mature.[23] The conventional WGS reaction is used to adjust the H_2/CO ratio of the syngas to satisfy the H_2/CO ratio requirement of DME synthesis. Because of the

low char yield in a pure steam biomass gasifier,[6] additional biomass serves as the fuel for combustion in addition to the char produced by the gasifier. Two CO_2 absorption facilities were designed, one for the syngas from the WGS and the other for flue gas from the combustor, both having similar designs and using diethanolamine (DEA) as the solvent. Because of the different CO_2 partial pressures and CO_2 concentrations, the heat consumptions for these two separation processes are different, being about 2.5 and 4.5 MJ/kg of CO_2, respectively. The clean syngas is sent to the synthesis reactor and converted to DME. The steam needed by gasification, WGS, CO_2 capture, and so on is provided through heat-recovering steam generation (HRSG) by both cooling the high-temperature syngas and flue gas and recovering the reaction heat from the DME synthesis section. Part of the electricity needed for this process can be generated by a steam turbine. To make the energy and exergy analysis more practical and clear, we divided the overall flowsheet into seven sections, with the boundary for each section being indicated by a dashed rectangle as shown in Figure 1. The numbers in circles refer to the main streams in this process.

3. Method

Based on Figure 1, we developed rational simulation models of the different units in the process depending on the literature data and research results, as well as the operating parameters from the industrial processs. The parameters were adjusted to optimize the mass and energy utilization efficiencies of the overall system. A detailed exergy analysis on the basis of the second law and the simulation results was performed so that the analysis and assessment were more comprehensive and practical. A detailed breakdown of the thermodynamic losses was performed, and thus, appropriate measures can be recommended to increase the efficiency of the process.

Some assumptions were made in this simulation work, as follows: (1) The biomass fed into the gasifier is treated, and the moisture content is 7.5 wt %; hence, no additional heat is necessary for biomass pretreatment. (2) In the gasifier, higher gasification temperature can greatly reduce unwanted methane formation. Because of the low content of methane (about ~2 wt % in syngas), a methane reforming unit is not included here. This small amount of methane produced can be separated from the system and mixed with the tail gas from DME synthesis to be used as combustion fuel. (3) The syngas produced by the gasifier contains various contaminants, including particles, condensable tar, alkali compounds, H_2S, HCl, NH_3, HCN, and COS depending on the different feedstocks and gasifiers.[8] However, it is difficult to collect or obtain data on all of these components for the selected biomass and process. Furthermore, the energy consumption and exergy loss of a gas cleaning process is relatively lower than that of the other process sections.[18] Thus, this work does not include a gas cleaning section. (4) A two-step DME synthesis technology is simulated in this work. The one-pass conversion rate of methanol and DME is no more than 70−80%, with recycling of unreacted reactants to ensure an overall conversion near 95%. (5) The energy consumption or exergy loss caused by heat transfer between the phase interface or the equipment walls and the fluid dynamics are not considered in this work.

3.1. Estimation of Exergy. 3.1.1. Estimation of Enthalpy of Formation of Biomass. The thermodynamic properties of biomass, such as the higher heating value (HHV) or lower heating value (LHV) and the standard enthalpy of formation of biomass, are essential for simulating the biomass gasifier and combustor. However, these thermodynamic properties are not exactly known because the structure of biomass is not well-defined; thus, the ordinary thermodynamic estimation models, such as UNIFAC, would not be effective. Statistical correlations based on experimental data are often used to resolve this problem. For instance, the HHV and the exergy of the organic fuels (e.g., biomass, coal, natural gas) can be accurately predicted by a correlation formula that is described in detail in the literature.[24]

For biomass, the standard enthalpy of formation, ΔH_f^0, in the standard state (usually 298 K, 1 atm) varies between the different types of biomass and cannot be obtained easily from handbooks. However, its combustion heat or heat value can be measured experimentally or estimated with a correlation formula. If one assumes the composition of the biomass to be $C_\alpha H_\beta O_\gamma N_\delta S_\varepsilon$, then based on the biomass combustion heat reaction

$$C_\alpha H_\beta O_\gamma N_\delta S_\varepsilon + \left(\alpha + \frac{\beta}{4} + \delta + \varepsilon - \frac{\gamma}{2}\right)O_2 \rightarrow \alpha CO_2 + \frac{\beta}{2}H_2O(\text{g or l}) + \delta NO_2(\text{g}) + \varepsilon SO_2(\text{g}) \quad \text{(I)}$$

the ΔH_f^0 value of the biomass can be calculated with the equation

$$\Delta H^0_{f,\text{biomass}} = -\Delta H^0_{\text{HHV}} + \alpha \Delta H^0_{f,CO_2(g)} + \frac{\beta}{2}\Delta H^0_{f,H_2O(l)} + \delta \Delta H^0_{f,NO_2(g)} + \varepsilon \Delta H^0_{f,SO_2(g)} \quad (1)$$

where α, β, γ, δ, and ε are the mole contents of the elements C, H, O, N, and S, respectively, obtained from the ultimate analysis of the biomass. The ΔH_f^0 values of CO_2(g), H_2O(l), NO_2(g), and SO_2(g) can be obtained from a handbook.

3.1.2. Exergy Calculation and Exergy Analysis. Exergy analysis is a widely used approach for analyzing and improving the efficiency of chemical and thermal processes. The exergy concept is a thermodynamic tool that expresses the quality of energy: it is the amount of work that can be obtained from a system when it is brought into equilibrium with the state of the environment. Unlike energy, exergy is consumed in all real-world processes as entropy is produced, making it the ultimate limiting resource for the functioning of all systems. The results of exergy and energy analyses can be similar or different, depending on the studied processes.[25] Energy can never be "lost" because it is conserved according to the first law of thermodynamics, whereas exergy can be lost as a result of internal irreversibilities; therefore, exergy losses should be minimized when striving for high energy utilization efficiency. Hence, combining exergy and energy analyses for a complicated process provides a comprehensive understanding of the energy utilization status and exergy loss, which is useful for improving the process design.

By definition, the exergy value of a stream can be divided into five important contributions, namely, kinetic exergy (c^2/2), potential exergy (gX), physical exergy (B_{ph}), chemical exergy (B_{ch}), and nuclear exergy (B_{nu}). The general expression for exergy is given by[24]

$$B = \frac{c^2}{2} + gX + B_{ph} + B_{ch} + B_{nu} \quad (2)$$

where g is the constant of gravitational acceleration, c is the velocity relative to Earth's surface, and X is the height. For a chemical process, the exergy value of a stream consists of mainly physical exergy and chemical exergy, and the other components can be neglected for most practical purposes. The environmental state is chosen as $T_0 = 25$ °C and $P_0 = 1$ atm,

which is same as the thermodynamic standard state. The phase state of water in the standard state is the liquid phase.

Exergy Calculation. Based on the mass and energy balances obtained from the process simulation, the physical exergy of a stream, B_{ph}^{st}, can be calculated as

$$B_{ph}^{st} = (H - H_0) - T_0(S - S_0) \quad (3)$$

where H and S are the enthalpy flow and entropy flow, respectively, of the stream and H_0 and S_0 are the enthalpy flow and entropy flow, respectively, of the stream under environmental state T_0 and P_0.

The chemical exergy of a stream, B_{ch}^{st}, can be calculated as

$$B_{ch}^{st} = F\tilde{B}_{ch} = F(\sum_i y_i B_{ch_i} + RT_0 \sum_i y_i \ln a_i) \quad (4)$$

where F is the molar flow rate of the stream, $\tilde{B}_{ch}$ is the specific chemical exergy of the stream, B_{ch_i} is the molar chemical exergy of the ith component, y_i is the molar fraction of the ith component in the stream, and a_i is the activity of the ith component in the stream.

The standard chemical exergy of a pure substance, $B_{ch_i}^0$, at the standard state (25 °C, 1 atm) can be obtained from the literature.[24,26] Because the environmental state is same as the standard state in this work, $B_{ch_i} = B_{ch_i}^0$. Equations 3 and 4 can also be used for calculating the exergy of steam or water. The exergy of electricity is same as its power value.

Exergy Loss. The exergy analysis is performed based on the exergy inputs and outputs of a unit or a process. The exergy loss, or the irreversibility, can then be found, and the corresponding improvement measures can be taken.[27−29] The exergy loss or irreversibility of a unit or a process is expressed in terms of the exergy balance as

$$I = \sum_{in} B_i^{st} - \sum_{out} B_j^{st} - B_Q + B_W \quad (5)$$

where I is the exergy loss of a unit or a process, $\sum_{in} B_i^{st}$ is the total exergy of the input streams of the unit or process, $\sum_{out} B_j^{st}$ is the total exergy of the output streams of the unit or process, B_Q is the exergy of heat exchange of the unit or process with the environment, and B_W is the exergy of the work performed by the unit or process

3.2. Modeling and Simulation. 3.2.1. Model of Biomass Steam Gasifier. The conversion of biomass to syngas in the steam gasification process is very high in the presence of a catalyst, such as dolomite or olivine. When the temperature is above 800 °C, the tar yield decreases to about 0.3 g/Nm^3 of dry gas, and the higher temperature reduces the methane formation. The suitable steam/biomass ratio is recommended to be 0.5−1.[6]

Because of the complexity of the biomass composition and the complicated reaction mechanism during biomass gasification, thermal pyrolysis, homogeneous gas-phase reactions, and heterogeneous gas−solid reactions can occur; therefore, establishing simulation models for gasification is a challenge. In this work, a quasi-equilibrium model was used for simulating the steam biomass gasification, and experimental data[6] were used to determine the suitable quasi-equilibrium temperature. Using a trial-and-error method, the suitable quasi-equilibrium temperature was found to be about 150−180 °C lower than the actual temperature. H_2, H_2O, CO, CO_2, and CH_4 were assumed to be the only stable gaseous components, and the calculated syngas composition agreed well with the literature.[6] We assumed a tar yield of 0 and a char yield of 30 g/kg of biomass based on literature data.[6,9] The steam/biomass ratio was set to be 0.6 (by mass), and the gasification was performed at atmospheric pressure and 880 °C.

Table 1. Ultimate Analysis of the Biomass Pellets and Other Properties[7]

Ultimate Analysis		
	wt % (mf)	mol %
C	50.7	30.62
O	42.4	19.21
N	<0.3	0.16
H by difference	6.9	50.01
Other Data		
moisture content (%, wt)	7.5	
ash content (%, mf)	0.39	
calorific value (MJ/kg raw pellets)	18.86	
bulk density (kg/m^3)	668	
pellet diameter (mm)	6	
pellet length (mm)	6−15	

Ultimate analysis results for wood pellets and other properties are listed in Table 1. Using eq 1, the standard enthalpy of formation for the selected biomass, $\Delta H_{f,biomass}^0$, was estimated to be −6.114 MJ/kg. Then, the heat duties of the gasifier and the combustor can be predicted exactly with thermodynamic models.

3.2.2. Model of Water−Gas Shift Process. The purpose of the water−gas shift is to adjust the H_2/CO ratio in the syngas by changing the steam feed and operating parameters for the Co−Mo-based catalyst. A detailed description of this process is given in the literature.[23] The water−gas shift reaction proceeds rapidly to a condition very near chemical equilibrium; thus, the isothermal equilibrium model was used for modeling this reaction, and the thermodynamic properties were estimated with the Peng−Robinson equation of state. The operating conditions in the shift reactor were assumed to be 240 °C and 10 bar. The steam fed into the shift reactor was adjusted to ensure that the H_2/CO ratio from the shift reactor would be 2.1−2.3 to satisfy the requirements for DME synthesis.

3.2.3. Model of Dimethyl Ether Synthesis Process. A two-step approach was used for synthesizing DME, as follows

$$CO + 2H_2 \rightleftarrows CH_3OH \quad (II)$$

$$2CH_3OH \rightleftarrows CH_3OCH_3\ (DME) + H_2O \quad (III)$$

Initially, methanol was synthesized with the syngas, and then the methanol was converted into DME and water. Methanol synthesis is an exothermic reaction that was conducted over a Cu-based catalyst (such as $CuO/ZnO/Al_2O_3$), at 220−260 °C and 20−40 bar, in a packed-bed reactor. To overcome the lower one-pass conversion efficiency of methanol synthesis, part of the unreacted gas was recycled to the reactor after being separated from the methanol product. A detailed flowsheet description and simulation study can be found in the literatures.[30,31] The methanol reactor was assumed to be an isothermal equilibrium reactor, and the Soave−Redlich−Kwong equation was used to describe the thermodynamic properties of this process.[32] The synthesis reaction of DME was performed with γ-Al_2O_3 as the catalyst and methanol as the feedstock. In the reactor, the pressure ranged from 10 to 20 bar, and the reaction temperature was approximately 300 °C. The one-pass conversion of methanol to DME was about 70−85%. Water and unreacted methanol were separated from the DME product, and the recovered methanol was then recycled to the DME reactor after

Table 2. Information on the Main Streams in the BSGtF Process

	stream no.										
	1	2	3	4	5	6	7	8	9	10	11
temp (°C)	25	880	150	93	60	25	80	25	354	120	60
pressure (bar)	1.32	1.32	1.32	10	10	20	200	1.82	1.82	1.82	20
mass flow (kg/h)	1	1.57	1.57	1.39	0.791	0.525	1.467	0.4	6.46	6.46	0.028
mass fraction											
CH_4	−	0.0181	0.0181	−	−	−	−	−	−	−	−
H_2	−	0.0665	0.0665	0.0809	0.1426	−	−	−	−	−	0.5563
O_2	−	−	−	−	−	−	−	−	0.091	0.091	−
H_2O	−	0.1415	0.1415	−	−	0.0039	0.0020	−	0.062	0.062	−
C	−	0	0	−	−	−	−	−	−	−	−
CO	−	0.5038	0.5038	0.4841	0.8536	−	−	−	−	−	−
CO_2	−	0.2682	0.2682	0.4328	−	−	0.9960	−	0.134	0.134	−
N_2	−	0.0019	0.0019	0.0022	0.0038	−	0.0020	−	0.713	0.713	0.1024
methanol	−	−	−	−	−	0.0036	−	−	−	−	0.3412
DME	−	−	−	−	−	0.9925	−	−	−	−	0
energy flow (MJ/h)	20.37	27.88	24.84	22.53	22.9	16.56	0.184	8.15	4.56	2.89	2.43
exergy flow (MJ/h)	21.39	23.32	21.79	20.58	20.33	16.16	1.029	8.56	1.92	1.24	2.09

Table 3. Overall Mass and Energy Balances for the BSGtF Process[a]

	mass flow (kg/h)	energy (MJ/h) (HHV)	exergy (MJ/h)
	Input		
biomass	1.4	28.52	29.95
air	6.0		
steam (gasifier, WGS)	0.68		
power		3.77	3.77
	Output		
DME product	0.525	16.56	16.16
CO_2 product (>99 wt %)	1.467	0.184	1.029
CO_2 free exhaust gas	5.59		
wastewater	0.458		
	Utility		
power demand (MJ/h)	3.77		

[a] Main operating parameters: Gasifier: 880 °C, 1.32 bar, steam/biomass ratio (mass) = 0.6. Combustion: 950 °C, 1.82 bar. Water−gas shift: 240 °C, 10 bar. Methanol synthesis: 240 °C, 25 bar. DME synthesis: 280 °C, 20 bar.

being mixed with the feedstock methanol. The Soave−Redlich−Kwong equation was used for the DME synthesis process, and the UNIQUAC-RK thermodynamic model was used for the separation process. The reaction heat in this process can be recovered to produce low-pressure steam.

3.3. Energy and Exergy Efficiency of the Process. η^{E}_{total} is defined as the energy conversion efficiency of biomass to fuel considering the higher heating values of the product ($E_{product\ fuel}$) and resource ($E_{biomass}$) and the power demand (W_{net}) as in eq 6. η^{B}_{total} is defined as the exergy conversion efficiency of biomass to fuel considering the exergy values of the product ($B_{product\ fuel}$) and resource ($B_{biomass}$) and the power demand (W_{net}) as in eq 7.

$$\eta^{E}_{total} = \frac{E_{product\ fuel}}{E_{biomass} + W_{net}} \times 100\% \quad (6)$$

$$\eta^{B}_{total} = \frac{B_{product\ fuel}}{B_{biomass} + W_{net}} \times 100\% \quad (7)$$

4. Results and Discussion

4.1. Overall Mass and Energy Balances. Based on Figure 1, the information about the main streams that connect the different sections in the total BSGtF process is collected in Table 2, and the overall mass and energy balances are listed in Table 3. Here, we take the calculation benchmark as 1 kg/h biomass feedstock because it simplifies comparisons and could be scaled up to the industrial scale without affecting the simulation results. The total energy efficiency, η^{E}_{total}, and the total exergy efficiency, η^{B}_{total}, from biomass to fuel were found to be 51.3% and 47.9%, respectively. In addition to the DME product, this process can also provide high-purity CO_2 product (200 bar) for CO_2 storage (2.8 tons of CO_2 is captured and compressed per ton of DME), resulting in a net CO_2 reduction in emissions to the atmosphere. However, the penalty is that additional power is needed for CO_2 capture and compression. The total energy and exergy efficiencies can increase to 53.4% and 49.8%, respectively, without CO_2 compression.

If the compressed CO_2 is regarded as another product, then the exergy of compressed CO_2 should be included in eq 7, which results in an increase in the total exergy efficiency from 43.5% to 51.0%.

4.2. Substance Flow Analysis. Substance flow analysis of a total process can reveal the distribution of the main substances involved in the process. It can show the flow of an element as it enters and leaves the region in the study, which can be used to estimate the losses and environmental impacts occurring during various processes and during the various stages of a process. In this work, we have focused on hydrogen and carbon, two vital elements that are contained in both the raw materials and the products.

4.2.1. Carbon Balance and Carbon Flow. Figure 2a shows the carbon flow of the BSGtF process. The carbon in this process comes from the biomass, both for gasification and for combustion. With the simulation results, 71.43% of the total carbon in the biomass is used for gasification, and the rest of the carbon is used for combustion. Of the total carbon amount, 67.19% is converted to raw syngas (i.e., CO, CO_2, and a small amount of CH_4). After the application of gas cleaning and the water−gas shift to the raw syngas, 63.94% of the total carbon flows to the CO_2 capture section, and 3.25% is emitted to the environment. In the CO_2 capture section, 23.06% of the total carbon, which exists as CO_2, is separated from the syngas and then sent to the CO_2 compressor. Finally, 38.47% of the carbon is converted into the DME product. On the combustion side, 33.1% of the total carbon existing in the form of CO_2 from the flue gas is captured and compressed. Thus, a total of 56.16% of the total carbon is converted into CO_2. About 6.37% of the total carbon is released to the environment in the form of wastewater and waste gas.

The preceding analysis indicates that the atom utilization efficiency of carbon to fuel in BSGtF is only 38.47%, and this low atom utilization efficiency is derived from the limitations

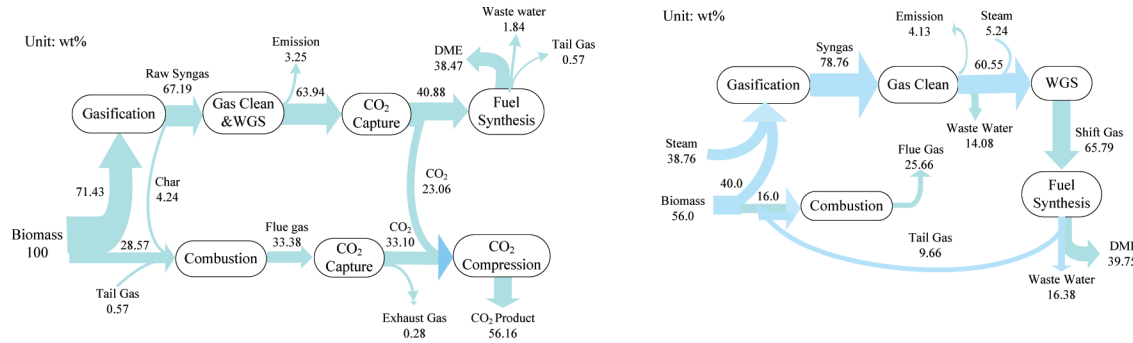

Figure 2. Schematic representation of the element balance and flow in the BSGtF process.

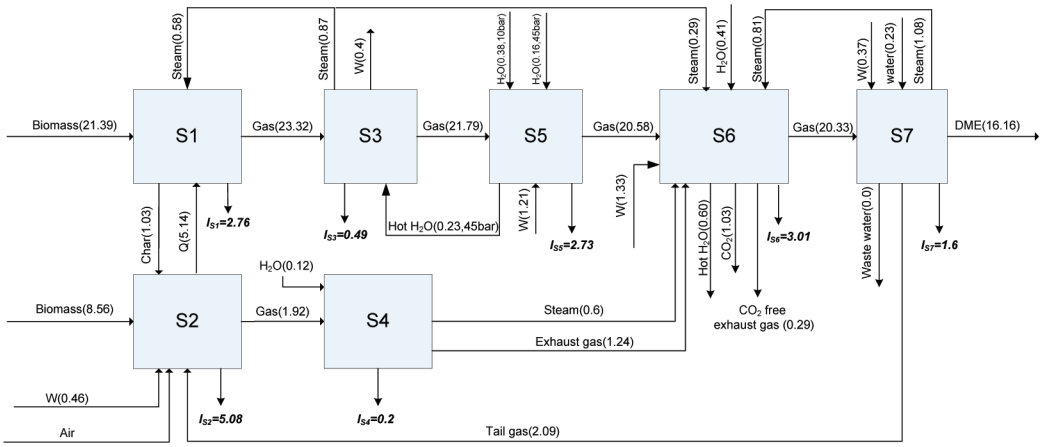

S1 – Gasification process; S2 - Combustion & air preheat; S3 - Heat recovery of raw syngas;

S4 - Heat recovery of combustion flue gas; S5 - Gas compression & water gas shift;

S6 — CO_2 capture & compression; S7 — DME synthesis

Figure 3. Exergy flows of the total BSGtF process.

of the steam gasification process itself. The current technology produces H_2 from the steam and biomass, while simultaneously, a large amount of carbon (~57% in this process) must be consumed and converted into CO_2 that will be captured or emitted to the environment. Therefore, if another H_2 resource could be available, such as from renewable solar power or hydropower, then the total carbon atom utilization could be improved greatly. On the other hand, the combustion process consumed a certain amount of biomass. If the heat for gasifying the biomass could be obtained from other energy resource, the carbon atom utilization could be increased greatly, and the CO_2 emissions could be decreased considerably.

4.2.2. Hydrogen Balance and Hydrogen Flow. Figure 2b shows the hydrogen balance and flow in the BSGtF process. The hydrogen comes from both the biomass and the gasification steam, which account for 56.0% and 38.76%, respectively, of the total hydrogen. In total, 39.75% of the total hydrogen is converted into the DME product, but about 56.12% of the hydrogen is lost as water byproduct, as well as small amounts of methanol and methane. Among the lost hydrogen, about 25.66% of the total hydrogen is consumed by the combustion process. Just as in the carbon flow analysis, the means of increasing the hydrogen atom efficiency from biomass to fuel is getting hydrogen from other energy resources and providing the heat needed for steam gasification in other ways.

4.3. Exergy Analysis of the Overall Process. Figure 3 shows the exergy flow of the total process from biomass to DME. The exergy losses in different sections are indicated by the letter I. S1 (gasification process) and S2 (combustion and air preheat) are two central units with larger exergy losses than the other sections. Detailed analysis and improvement measures for these processes are provided in section 4.4. S5 (gas compression and WGS) has a moderate exergy loss, which is caused by interstage cooling of the compressor, unrecovered heat rejected to the environment by the cooling mechanism, and intrinsic losses caused by the WGS reaction. S6 (CO_2 capture and compression) also has a moderate exergy loss, because, in addition to the power for CO_2 compression, a large amount of low-pressure steam is consumed to regenerate the rich amine solution. Considering the CO_2-free exhaust gas as a discharge to the environment (i.e., assuming no use for this exhaust gas), the exergy efficiency in S6 (CO_2 capture and compression) would decrease from 88.1% to 86.9%. This part of the exergy loss can be reduced by using oxygen-rich combustion, but additional energy is then required for air separation. In S7 (DME synthesis), reaction heat is recovered to produce low-pressure steam, so the exergy loss is mainly derived from the intrinsic synthesis reaction and the wastewater discharged from the system, which is hard to avoid. The exergy losses in S3 (heat recovery of raw syngas) and S4 (heat recovery of combustion

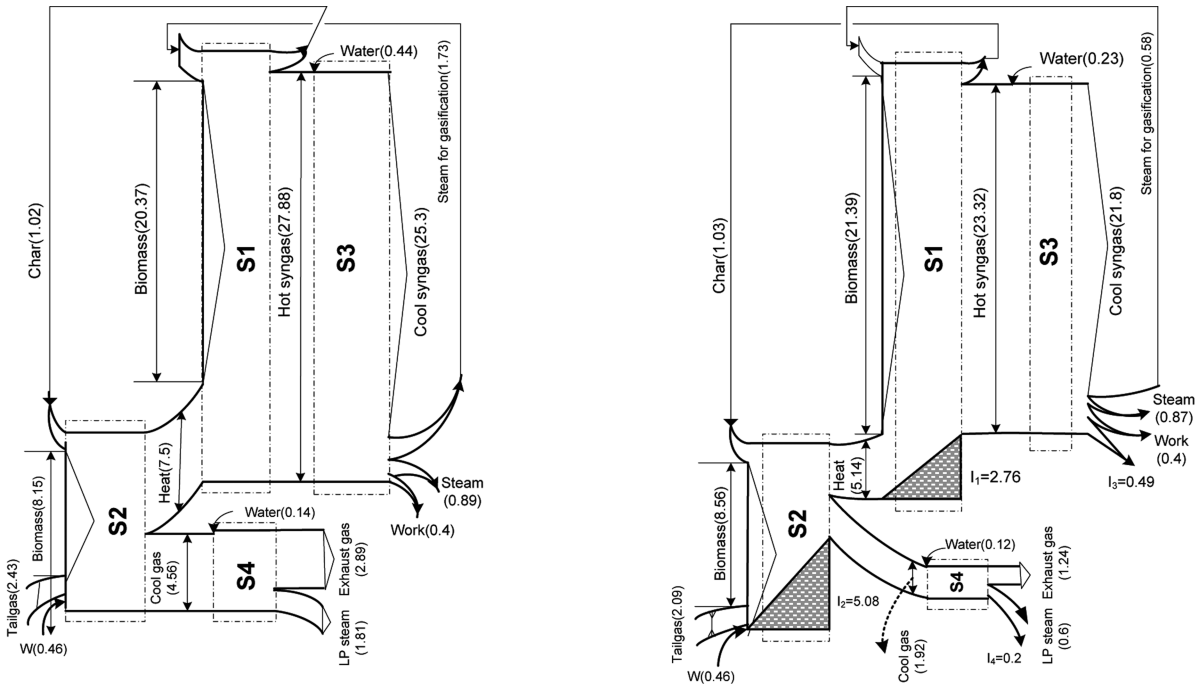

Figure 4. Energy and exergy flow diagrams of the integrated gasifier and combustor.

flue gas) are primarily produced by the irreversibility due to heat transfer over a finite temperature, and they are relatively small and cannot be reduced much.

4.4. Exergy Analysis of Integrated Gasifier and Combustor. Figure 4 shows the energy and exergy flow diagrams of the integrated gasifier and combustor, as well as two heat recovery systems (S1−S4 in Figure 1). About 28.6% of the total biomass feedstock is combusted to provide the heat needed for the endothermic steam gasification reaction. The combustion temperature should be higher than the gasification temperature in order to transfer the heat to the gasifier using sand as the heat medium. Increasing the temperature difference between the combustor and the gasifier will increase the heat-transfer rate, but the exergy loss caused by the heat transfer will be increased too, as discussed in section 4.4.2.

The exergy loss of the gasifier is caused by the reactions tha decompose the large biomolecules, such as cellulose, hemicellulose, and lignin, into smaller gas molecules. The heat from the combustor can provide energy for this decomposition. The total exergy efficiency of gasification is as high as 89.8%, which means that steam gasification is a high-exergetic-efficiency process. Because the present exergy loss is primarily caused by the intrinsic irreversibility, further improvement would be difficult to obtain. Other forms of irreversibility, such as fluid dynamic losses, heat losses, and so on, probably lead to further degradation of the energy and need to be considered in the future.

Combustion is a complex process composed of several irreversible steps: mixing of the fuel with the oxidizer, chemical reaction, heat transfer from the reacting molecules to other molecules, mixing of combustion products with remaining parts of combustion gases, and so on. Preheating of the reactants is the most common way of reducing the irreversibility of a combustion process. Increasing the air feed temperature means that much more heat can be recovered in the flue gas and that the amount of biomass required for combustion can be reduced. However, it will result in less low-pressure steam production in the HRSG. Without considering the heat loss and incomplete combustion, the exergy efficiency of the combustor is 58.2%, which indicates that combustion is a low-exergetic-efficiency process as compared to gasification whose total exergetic efficiency is 89.8%. In addition to changing the combustion conditions to improve the energy utilization efficiency, other ways to provide the heat needed by gasification should also be considered.

For heat exchanges in S3 (heat recovery of raw syngas) and S4 (heat recovery of combustion flue gas), we consider only the irreversibility due to heat transfer over a finite temperature difference, so the exergy losses cannot be avoided.

4.4.1. Influence of Gasification Temperature on the Performance of the Gasification Process. Figure 4 shows the influence of the gasification temperature on the gasification performance. The energy efficiency, $\eta^{E}_{gasification}$, and the exergy efficiency, $\eta^{B}_{gasification}$, of gasification can be estimated by the equations

$$\eta^{E}_{gasification} = \frac{HHV_{syngas}}{HHV_{biomass} + HHV_{steam} + Q_{gasification}} \times 100\% \quad (8)$$

$$\eta^{B}_{gasification} = \frac{B_{syngas}}{B_{biomass} + B_{steam} + B_{Q,gasification}} \times 100\% \quad (9)$$

where $Q_{gasification}$ is the heat transferred from the combustor and its exergy value, $B_{Q,gasification}$, can be calculated as $Q(1 - T_0/T_{gasifier})$. HHV_{syngas} refers to the higher heating value of cold syngas.

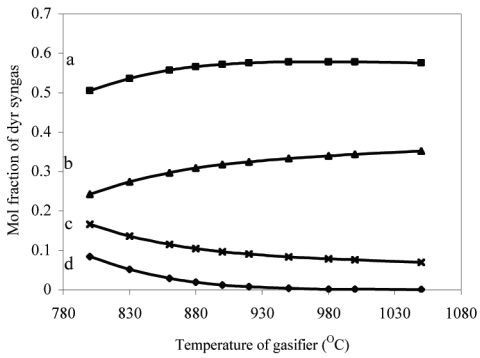

(i) Dry gas composition

a) H_2; b) CO; c) CO_2; d) CH_4

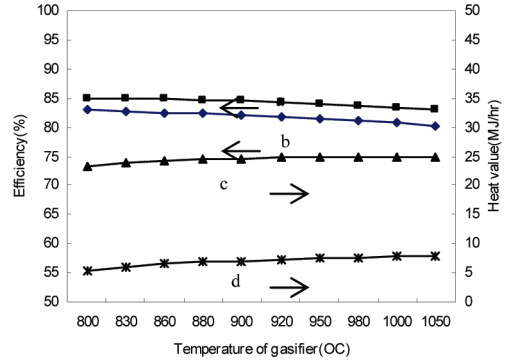

(ii) Gasification efficiencies and heat value of syngas

a) Energy efficiency of gasification; b) Exergy efficiency of gasification; c) High heat value of syngas; d) Gasification heat

Figure 5. Influence of gasification temperature on the performance of the gasifier [steam/biomass ratio = 0.6 (by mass), feed biomass = 1 kg/h].

Figure 5i shows that, with increasing gasification temperature, the H_2 content in the syngas increases, and the CH_4 content decreases. This means that a higher temperature can promote the methane steam reforming reaction in the gasifier, yielding syngas with low methane content, which is desirable for further transportation fuel synthesis. However, this tendency becomes weak when the temperature is above 900 °C. In addition, a decrease in CO_2 content can improve the H_2 and CO yields and, consequently, increase the heating value of the produced syngas (as shown in Figure 4ii, curve c). However, the penalty is that much more heat is needed for gasification (Figure 5ii, curve d). Moreover, because the temperature has a relatively weak effect on the heating value and chemical exergy of the syngas, the net result of improving the gasification temperature results in slight decreases in the energy efficiency (Figure 5ii, curve a) and exergy efficiency (Figure 5ii, curve b). This result is partly supported by the theoretical thermodynamic analysis of biomass gasification in the literature.[17] Thus, the suitable temperature should be traded off based on the simulation results. Furthermore, Figure 5 also shows that the lower heating value of dry syngas reaches about 16.4 MJ/kg (at 900 °C), which confirms the advantage of steam biomass gasification in providing a medium-heating-value gas product.

4.4.2. Influence of Combustion Temperature on the Gasification Process. Combustion temperature is often considered as a critical parameter affecting exergy efficiency. For a real industrial biomass gasification process, high combustion temperature often results in agglomeration because of the biomass potassium interacting with the silicate compounds. One effective way to address this problem is to add a small amount of MgO to avoid the formation of glasslike bed agglomerations, so that the combustion temperature can be higher than 1000 °C.[11] In this work, we selected a combustion temperature range for calculation of 900−1200 °C. Figure 6 shows the influence of the combustion temperature on the gasification process. Curve a refers to the total exergy efficiency of the combustor with increasing combustion temperature. This means increasing the combustion temperature can increase the exergy efficiency. The main reason for this result is that the higher-temperature flue gas can preheat the air to a higher temperature (Figure 6, curve c) and increase its exergy, so that the irreversibility of the combustion process can be reduced. However, for this indirectly heated biomass gasification process, the hot sand medium will transfer heat from the combustor to the gasifier.

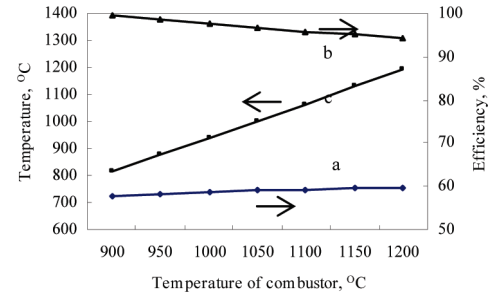

Figure 6. Influence of combustion temperature on the gasification process.

If one considers the combustor and gasifier as two thermal energy reservoirs, at temperatures of $T_{\text{combustor}}$ and T_{gasifier}, respectively, with $T_{\text{combustor}} > T_{\text{gasifier}}$, when heat transfer Q takes place between the two reservoirs over a finite temperature difference, the exergy efficiency of heat transfer can be calculated as

$$\eta^{\text{B}}_{\text{transfer}} = \left[1 - \left(\frac{T_0}{T_{\text{gasifier}}} - \frac{T_0}{T_{\text{combustor}}}\right)\right] \times 100\% \qquad (10)$$

Based on eq 10, assuming that the gasification temperature is fixed, then increasing the combustion temperature will decrease the exergy efficiency of the heat-transfer process, as shown in Figure 6, curve b. Thus, a rational combustion temperature should be determined considering both the gasification temperature required and the exergy efficiency of the combustor, as well as the transfer temperature difference between them.

4.5. Effects of Temperature and Steam/Biomass Ratio on the DME Yield. Figure 7 shows the effects of temperature and the steam/biomass ratio (R) in the gasifier on the DME yield. Increasing the steam/biomass ratio and the gasification temperature can improve the product yield of the fuel, but when the temperature is above 950 °C, the effect of the temperature become weak. Combining these results with those of Figure 5ii, the resulting disadvantage is that the exergy and energy efficiencies in the gasifier are reduced slightly. Thus, the optimal temperature range can be set from 900 to 1000 °C. With a higher steam/biomass ratio, the DME yield increases by increasing the H_2 concentration and lowering the CO_2 concentration in the gas product, but the steam demand for gasification increases as well.

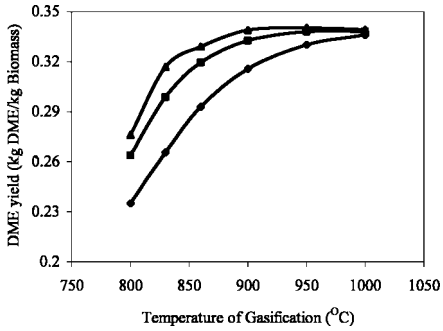

Figure 7. Effects of temperature and steam/biomass ratio (R) of the gasifier on the DME yield.

The effect of the steam/biomass ratio on the DME product output becomes weaker at higher gasification temperatures. A rational steam/biomass ratio range is recommended as 0.6−0.8.

5. Conclusions

A flowsheet for producing the substitutable transport fuel dimethyl ether through biomass steam gasification (BSGtF) was constructed including heat integration. The total flowsheet was divided into seven sections in order to understand deeply the mechanism of the material and energy conversions occurring during the process. A quasi-equilibrium model was applied to simulate the gasifier, and the rational quasi-equilibrium temperature was identified. The predicted syngas composition agreed well with the experimental data reported in the literature. A formula to calculate the standard enthalpy of formation of a biomass sample was proposed and applied to ensure a more reliable energy balance analysis for biomass gasification and combustion. The mass and energy balances for each section and the total flowsheet and the carbon and hydrogen flows of the process were calculated from the process simulation results. The exergy flows of the overall process and the exergy losses in each section were obtained according to the second law.

The research indicated that the total energy and exergy efficiencies from biomass to fuel are 51.3% and 47.9%, respectively, and that the CO_2 emission effect is negative (2.8 tons of CO_2 is captured and compressed per ton of DME product). The energy and exergy efficiencies can reach 53.4% and 49.8%, respectively, without including the electricity consumption for CO_2 compression. If the compressed CO_2 is regarded as another product, then the exergy of compressed CO_2 should be included in eq 7, which results in an increase in the total exergy efficiency from 47.9% to 51.0%.

In this BSGtF process, the gasifier and combustor are two central units. Their exergy efficiencies are 89.8% and 58.2%, respectively. The analysis indicated that these exergy losses are mainly caused by intrinsic irreversibility. Optimizing some parameters, such as gasification temperature, combustion temperature, and steam/biomass ratio, or applying some other measures, such as preheating the air into the combustor, could improve the exergy efficiencies. This work applied more rigorous thermodynamic models to simulate biomass gasification and combustion than has yet been resolved by current commercial software. In the present work, we divided the total flowsheet into seven sections, but much more detailed energy and exergy analyses should be performed within each section, focusing on heat exchange, heat loss, equipment configuration, and more refined unit models. Such studies, which will be the focus of future work in our group, can reveal more causes of exergy losses and provide more improvement possibilities.

Acknowledgment

This research was funded by Statoil Mongstad. We thank Sørum Lars for discussions of biomass gasification and providing valuable reference material. We also thank Johan E. Hustad for meaningful suggestions, as well as Ivar Ståle Ertesvåg and Anita Zvolinschi for fruitful discussions on exergy analysis. This work was also supported by the National Natural Science Foundation of China (No. 20676135) and the National Basic Research Program of China (973 Program, 2009CB219907).

Literature Cited

(1) Shinnar, R.; Citro, F. Energy−A road map to U.S. decarbonization. *Science* **2006**, *313* (5791), 1243–1244.

(2) Larson, E. D.; Consonni, S.; Katofsky, R. E.; Iisa, K.; Frederick, W. J. *A Cost−Benefit Assessment of Gasification-Based Biorefining in the Kraft Pulp and Paper Industry: Volume 1 Main Report*; Princeton University: Princeton, NJ, 2006.

(3) Larson, E. D.; Consonni, S.; Katofsky, R. E.; Iisa, K.; Frederick, W. J. *A Cost−Benefit Assessment of Gasification-Based Biorefining in the Kraft Pulp and Paper Industry: Volume 2 Detailed Biorefinery Design and Performance Simulation*; Princeton University: Princeton, NJ, 2006.

(4) Fossum, N. E. N. Biomass gasification combustion of mixtures. Ph.D. Thesis, Norwegian University of Science and Technology (NTNU), Trondheim, Norway, 2002.

(5) Sørum, L. Environmental aspects of municipal solid waste combustion. Ph.D. Thesis, Norwegian University of Science and Technology (NTNU), Trondheim, Norway, 2000.

(6) Rapagna, S.; Jand, N.; Kiennemann, A.; Foscolo, P. U. Steam-gasification of biomass in a fluidised-bed of olivine particles. *Biomass & Bioenergy* **2000**, *19* (3), 187–197.

(7) Barrio, M. Experimental investigation of small-scale gasification of woody biomass. Ph.D. Thesis, Norwegian University of Science and Technology (NTNU), Trondheim, Norway, 2002.

(8) Tijmensen, M. J. A.; Faaij, A. P. C.; Hamelinck, C. N.; van Hardeveld, M. R. M. Exploration of the possibilities for production of Fischer−Tropsch liquids and power via biomass gasification. *Biomass Bioenergy* **2002**, *23* (2), 129–152.

(9) Dupont, C.; Boissonnet, G.; Seller, J. M.; Gauthier, P.; Schweich, D. Study about the kinetic processes of biomass steam gasification. *Fuel* **2007**, *86* (1−2), 32–40.

(10) Paisley, M. A.; Litt, R. D.; Overend, R. P.; Bain, R. L. Gas turbine power generation from biomass gasification. In *ASME Cogen Turbo Power '94*; ASME Press: New York, 1994; pp 625−629.

(11) Spath, P.; Aden, A.; Eggeman, T.; Ringer, M.; Wallace, B.; Jechura, J. *Biomass to Hydrogen Production Detailed Design and Economics Utilizing the Battelle Columbus Laboratory Indirectly-Heated Gasifier*; Technical Report NREL/TP-510-37408; National Renewable Energy Laboratory: Golden, CO, 2005.

(12) Rozovskii, A. Y.; Slivinskii, E. V.; Lin, G. I.; Makhlin, V. A.; Kolbanovsky, Y. A.; Plate, N. A. Ecologically benign motor fuels and petrochemicals from alternative raw materials. *Pure Appl. Chem.* **2004**, *76* (9), 1735–1747.

(13) Wilhelm, D. J.; Simbeck, D. R.; Karp, A. D.; Dickenson, R. L. Syngas production for gas-to-liquids applications: Technologies, issues and outlook. *Fuel Process. Technol.* **2001**, *71* (1−3), 139–148.

(14) Hidaka, Y.; Sato, K.; Yamane, M. High-temperature pyrolysis of dimethyl ether in shock waves. *Combust. Flame* **2000**, *123* (1−2), 1–22.

(15) Zhang, L.; Huang, Z. Life cycle study of coal-based dimethyl ether as vehicle fuel for urban bus in China. *Energy* **2007**, *32* (10), 1896–1904.

(16) Zainal, Z. A.; Ali, R.; Lean, C. H.; Seetharamu, K. N. Prediction of performance of a downdraft gasifier using equilibrium modeling for different biomass materials. *Energy Convers. Manage.* **2001**, *42* (12), 1499–1515.

(17) Prins, M. J.; Ptasinski, K. J.; Janssen, F. J. J. G. From coal to biomass gasification: Comparison of thermodynamic efficiency. *Energy* **2007**, *32*, 1248–1259.

(18) Prins, M. J.; Ptasinski, K. J.; Janssen, F. J. J. G. Exergetic optimization of a production process of Fischer−Tropsch fuels from biomass. *Fuel Process. Technol.* **2004**, *86* (4), 375–389.

(19) Ptasinski, K. J.; Prins, M. J.; Pierik, A. Exergetic evaluation of biomass gasification. *Energy* **2007**, *32* (4), 568–574.

(20) Channiwala, S. A.; Parikh, P. P. A unified correlation for estimating HHV of solid, liquid and gaseous fuels. *Fuel* **2002**, *81* (8), 1051–1063.

(21) Li, X.; Grace, J. R.; Watkinson, A. P.; Lim, C. J.; Ergudenler, A. Equilibrium modeling of gasification: A free energy minimization approach

and its application to a circulating fluidized bed coal gasifier. *Fuel* **2001**, *80* (2), 195–207.

(22) Craig, K. R.; Mann, M. K. *Cost and Performance Analysis of Biomass-Based Integrated Gasification Combined-Cycle (BIGCC) Power Systems*; Technical Report NREL/TP-430-21657; National Renewable Energy Laboratory: Golden, CO, 1996.

(23) Gunardson, H. *Industrial Gases in Petrochemical Processing*; Marcel Dekker: New York, 1998.

(24) Szargut, J. *Exergy Method: Technical and Ecological Applications*; WIT Press: Southampton, U.K., 2005.

(25) Dewulf, J.; van Langenhove, H.; van de Velde, B. Exergy-based efficiency and renewability assessment of biofuel production. *Environ. Sci. Technol.* **2005**, *39* (10), 3878–3882.

(26) Kotas, T. J. *The Exergy Method of Thermal Plant Analysis*; Krieger Publishing Company: Malabar, FL, 1995.

(27) Geuzebroek, F. H.; Schneiders, L. H. J. M.; Kraaijveld, G. J. C.; Feron, P. H. M. Exergy analysis of alkanolamine-based CO_2 removal unit with AspenPlus. *Energy* **2004**, *29*, 1241–1248.

(28) Zvolinschi, A. Exergy analysis and entropy production minimisation in industrial ecology. Ph.D. Thesis, Norwegian University of Sciences and Technology (NTNU), Trondheim, Norway, 2006.

(29) Ertesvag, I. S.; Kvamsdal, H. M.; Bolland, O. Exergy analysis of a gas-turbine combined-cycle power plant with precombustion CO_2 capture. *Energy* **2005**, *30* (1), 5–39.

(30) Ballman, S. H.; Gaddy, J. L. Optimization of methanol process by flowsheet simulation. *Ind. Eng. Chem. Process Des. Dev.* **1977**, *16* (3), 337–341.

(31) Ing, W. H. Gasifier to methanol plant. Ph.D. Thesis, The University of Queensland, Brisbane Australia, 2004.

(32) Chang, T.; Rousseau, R. W.; Kilpatrick, P. K. Methanol synthesis reactions—Calculations of equilibrium conversions using equations of state. *Ind. Eng. Chem. Process Des. Dev.* **1986**, *25* (2), 477–481.

Received for review February 4, 2009
Revised manuscript received August 6, 2009
Accepted October 15, 2009

IE900199E